Supplementary information for

Interfacial rheology of linearly growing polyelectrolyte multilayers at the water-air interface: from liquid to solid viscoelasticity

Stéphane Pivard,[a] Leandro Jacomine,[a] Felix S. Kratz,[b] Catherine Foussat,[a] Jean-Philippe Lamps,[a] Mélanie Legros,[a] Fouzia Boulmedais,[a] Jan Kierfeld,[b] François Schosseler[a] and Wiebke Drenckhan*[a]

[a] *Institut Charles Sadron, CNRS UPR22 - Université de Strasbourg, France*
[b] *Department of Physics, TU Dortmund University, 44221 Dortmund, Germany*

Contents

S1. NaPSS characterisation

Size Exclusion Chromatography

The SEC set-up consists in a set DIONEX Ultimate 3000 (degasing device, pump, sample distribution), a differential refractometer OPTILAB rEX (Wyatt Techn.) and a multi-angle light scattering detection unit DAWN HELEOS II (Wyatt Techn.). It is equipped with 4 separation columns Shodex OH-pak 30 cm (802.5HQ, 804HQ, 806HQ, 807HQ) and one pre-column. The separation range is 500 to 10^9 g/mol. The eluant is 60% Millipore water + 40% acetonitrile + 0.1 M $NaNO_3$ with a flow rate of 0.5 mL/min. The solution was prepared 24 h in advance and filtrated with a 0.45 μm Millex filter (Millipore) before the injection. Fig. S1 shows the resulting chromatograms together with the molecular weight distribution calculated in the range where refractometry and light scattering signals are both measurable. The molecular weights were calculated by Zimm angular extrapolation through the values measured at all angles. The weight-averaged molecular weight of the sample is 77800 g/mol and the polydispersity index is 1.9.
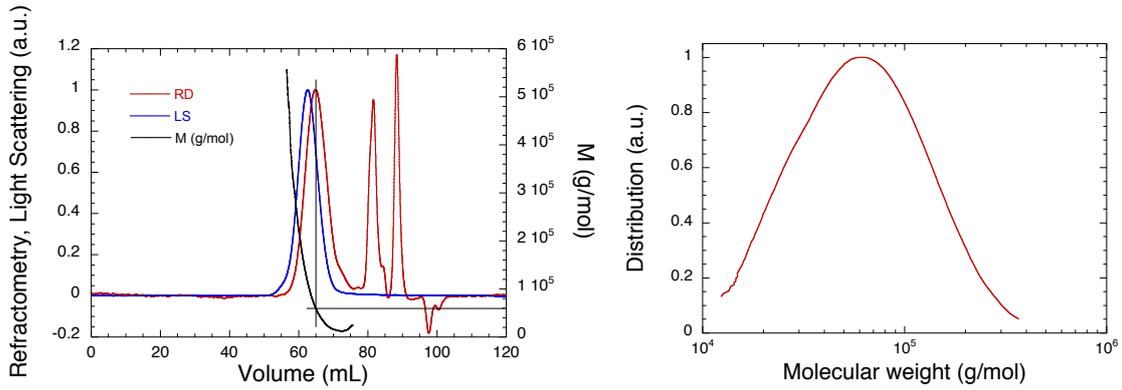

Figure S1. *SEC chromatograms (left) and molecular weight distribution (right) of the NaPSS sample.*

Degree of sulfonation

The degree of sulfonation of the NaPSS was estimated by two methods. First, elemental analysis gave the weight fraction of sulfur $w_S = 0.137_5$. It is related to the sulfonation degree x_S by

$$w_S = \frac{x_S m_S}{x_S m_{StS} + (1 - x_S) m_{St}} \tag{1}$$

where m_S, m_{St} and m_{StS} are the molecular weight of sulfur, styrene monomer and styrene sulfonate monomer, either in its salt form (m_{StS} = 206.7 g/mol) or acidic form (m_{StS} = 188.2 g/mol). Assuming that all sulfonate groups are in the salt form, this yields $x_S \approx 0.79_7$. With the unrealistic assumption that all sulfonate groups are in their acidic form the same value of w_S would give $x_S \approx 0.69_8$.

We also performed ^{1}H NMR analysis of the polymer in D_2O (Fig. S2). The peaks at $\approx$ 1.5 ppm and in the range 6 - 8 ppm correspond respectively to aliphatic and aromatic hydrogens. Their respective areas are given in the figure. The corresponding sulfonation degree depends on the way analysis is done.

For unsulfonated polystyrene, the ratio R of the aliphatic peak area to the aromatic peaks area should equal their stoichiometric ratio 0.6 while it should be 0.75 for fully sulfonated polystyrene. The sulfonation degree x_S is simply given by a linear interpolation between these two extreme cases,

$$R = 0.6(1 - x_S) + 0.75 x_S = 0.6 + 0.15 x_S \tag{2}$$

In an other approach, we can reason only on the aromatic hydrogens, after having calibrated the contribution of one hydrogen atom from the aliphatic peak area, which corrresponds to the contribution of 3 H. Using this calibration, we can calculate that the two peaks of the aromatic group in the range 6 - 8 ppm correspond to $\bar{n}_H$ = 3×4.178/2.923 = 4.288 H atoms. This average number of H atoms in the aromatic ring is related to the sulfonation degree x_S by

$$\bar{n}_H = 5(1 - x_S) + 4 x_S = 5 - x_S \tag{3}$$

Using Eq. (2), we get $x_S \approx 0.66_4 \pm 0.09_3$ while Eq. (3) yields $x_S \approx 0.71_2 \pm 0.08_6$. The errors have been calculated by assuming a relative integration error on each peak area equal to $\delta \approx 0.01$. They are slightly smaller in the second method, $\Delta x_S \approx 2\bar{n}_H \delta$, than in the first one, $\Delta x_S \approx 2R\delta/0.15$. Finally we can also use directly the peak area at 7.5 ppm, corresponding to protons linked to C atoms 3, 4 and 5 in the phenyl ring to obtain $x_S = 0.82_2 \pm 0.04$ or $x_S = 0.76_5 \pm 0.04$, depending wether the contribution of the protons is calibrated with the peak at 6.5 ppm or with the peak of the aliphatic hydrogen atoms, respectively. All these estimations are polluted by the small signal at about 7.1 ppm and the error δ is likely larger than 0.01.

To conclude, our NaPSS sample is clearly not fully sulfonated, with a value x_S likely around 0.75, which explains its amphiphilic behaviour.
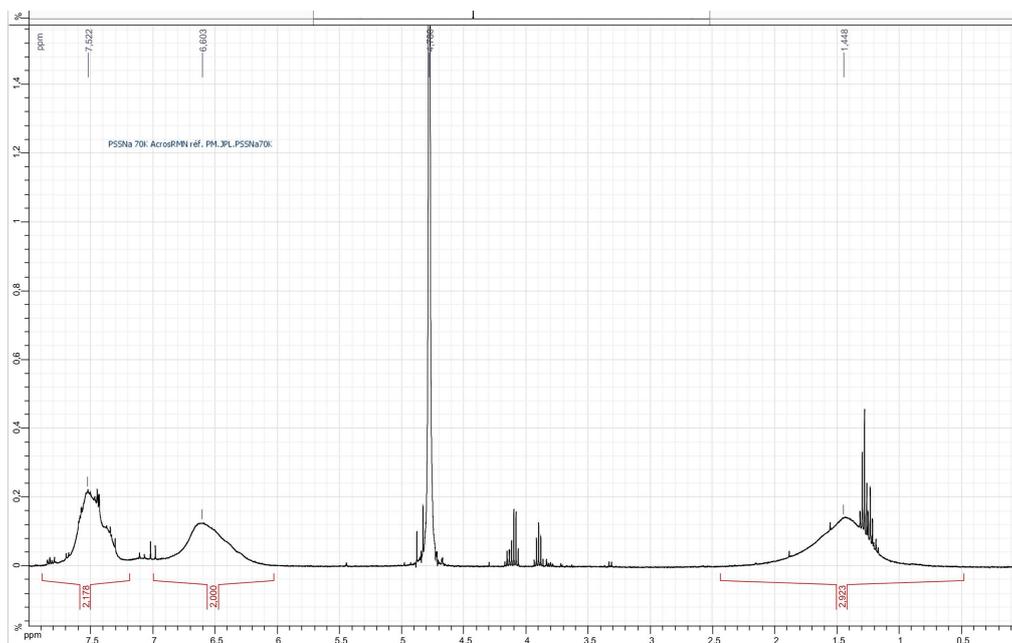

Figure S2. ^1H NMR of the NaPSS sample.
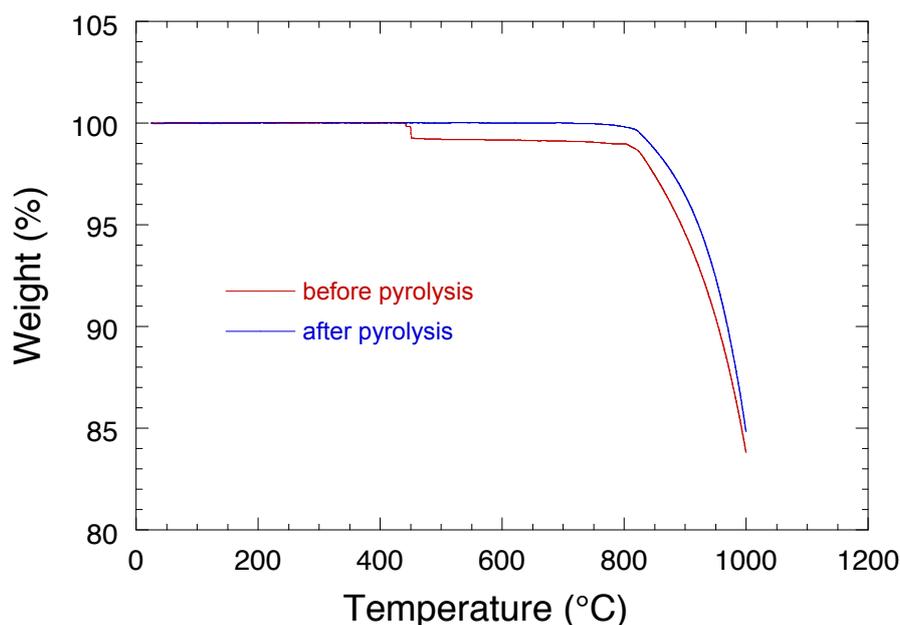
S2. Thermogravimetric analysis of NaCl

Figure S3. *TGA analysis of NaCl before and after baking at 600°C in an oven.*

Following Théodoly *et al*[1], we baked our salt in an oven at 600°C. Fig. S3 shows the thermogravimetric curves of the salt as received and after oven pyrolysis. This processing removes organic impurities (about 1%) that are eliminated at about 450°C. The measurements have been done with a TGA 2 instrument (Mettler Toledo). The mass of the sample was about 20 mg and the heating rate was 10°C/min under an air flow of 100mL/min.
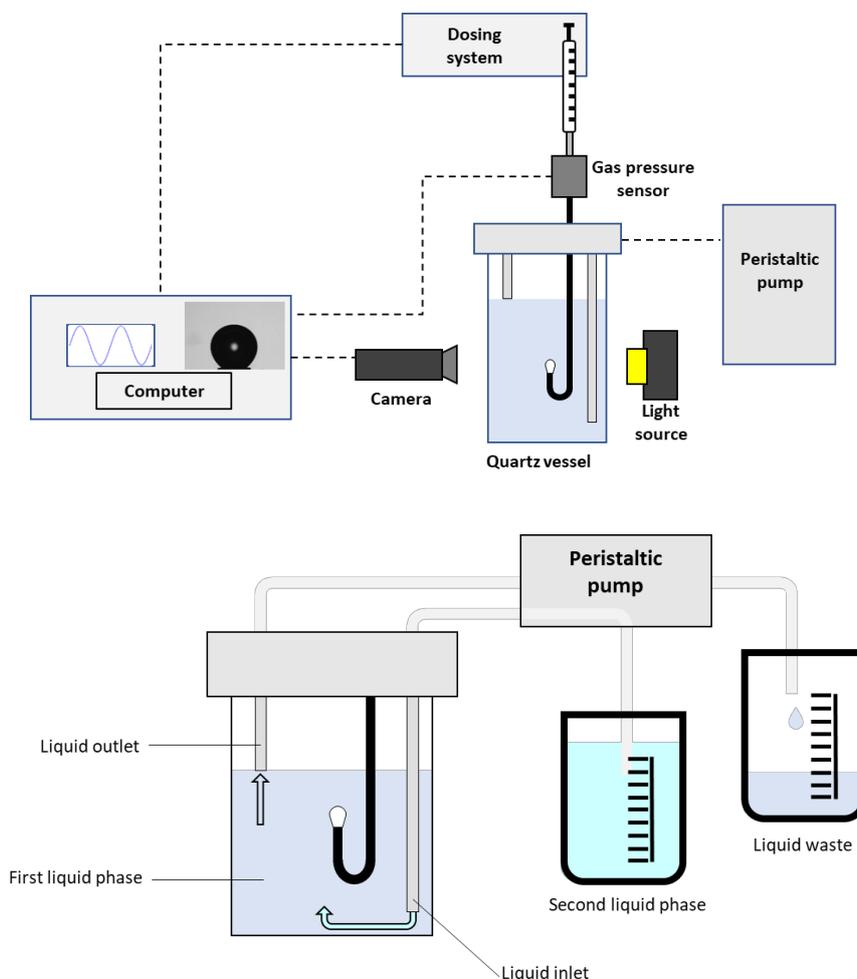
S3. Scheme of the tensiometry set-up

Figure S4. *Scheme of the different parts of our tensiometer.*

S4. Determination of ΔP

The pressure sensor measures the inner pressure of the bubble P_{in} relatively to the atmospheric pressure. This pressure includes the contribution of the water column above the bubble which can be easily measured. As a first approximation, in pure water, a difference of 0.1 mm on h_L (Fig. S5) corresponds to a variation of about 1 Pa in P_{in}, which yields a difference about 0.5-1mN/m in the effective interfacial tension γ_{eff} for our small bubbles with an apex radius value about 1.1 mm.

To calibrate the measurement of P_{in} we perform a preliminary experiment by deflating/inflating rapidly a bubble in the solution of NaPSS immediately after its creation. At this time, the Young-Laplace can still be used to measure the interfacial tension. We have the set of equations
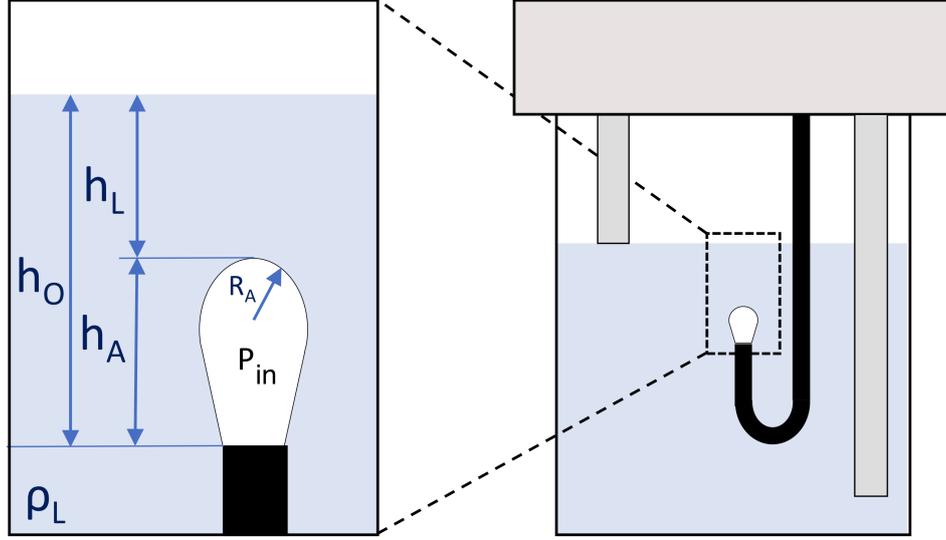
Figure S5. *Scheme of a bubble with the relevant variables for pressure measurements.*

$$\Delta P = P_{in} - P_{out} = \frac{2\gamma}{R_A} \tag{4a}$$

$$P_{in} = \rho_L g h_L + \frac{2\gamma}{R_A} \tag{4b}$$

$$h_L = h_0 - h_A \tag{4c}$$

where γ, R_A and h_A are respectively the surface tension, the radius of curvature of the apex and the height of the bubble. All these quantities are provided by the software of the tensiometer while the density of the liquid, ρ_L, is measured with a densimeter (Mettler-Toledo). Combining these equations, we get

$$P_{in} = \frac{2\gamma}{R_A} - \rho_L g h_A + \rho_L g h_0 \tag{5}$$

Equation (5) shows a linear relationship with slope 1 between the measured quantities P_{in} and $\frac{2\gamma}{R_A} - \rho_L g h_A$. Plotting the first versus the second, we obtain the intercept $\rho_L g h_0$ and thus we can easily calculate ΔP as

$$\Delta P = P_{in} - \rho_L g (h_0 - h_A) \tag{6}$$

In practice, we use the data obtained during the two steps of deflation and inflations and we average the two values of the intercept. Care is exercised to keep the height h_0 constant during the whole experiment, by using a large syringe (500 μL) that does not need a refill during the experiment and by a two-channels peristaltic pump to maintain a constant liquid height during the exchange of the surrounding liquid phase.

S5. Correction of ΔP shifts

Figure S6 (top left) shows a typical example of small shifts in $\gamma_{eff} = R\,\Delta P/2$ that we can observe occasionally during the oscillatory measurements performed on a bubble. They are in fact due to corresponding shifts in ΔP, which are possibly due to the fact that the peristaltic pump is switched off during the measurements and that the height of liquid is then no longer controlled. These shifts prevent a good averaging of the oscillatory signal and we correct them by calculating a shifting average of the signal over one period. The resulting values are then interpolated (black line) and we correct the experimental values as

$$\gamma_{eff,\,corr} = \gamma_{eff} - g(t) + <g(t)> \tag{7}$$

where $g(t)$ is the interpolation curve. The result is shown in Figure S6 (top right). The corrected data are then averaged while excluding those from the first and last oscillations (Fig. S6 , bottom plot).
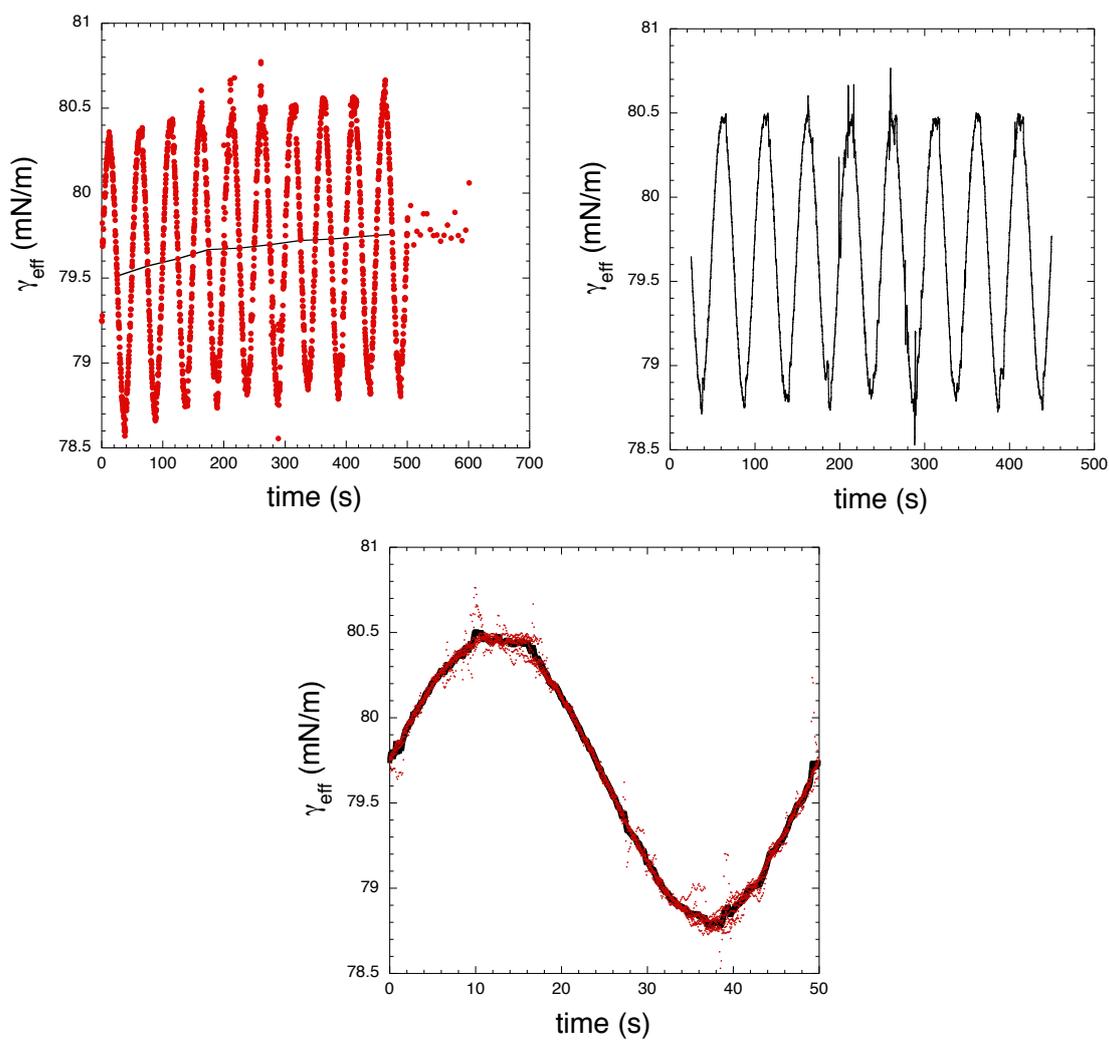
Figure S6. *Example of an experimental shift in γ_{eff} (left), of the data corrected with Eq. 7 (top right), and of the average (thick black line) obtained from the corrected data (red points) (bottom).*

The same correction is applied to data collected during the relaxation of the first NaPSS layer but in this case no averaging is performed afterwards and the GSD analysis is performed on each oscillation. This explains larger scattering in the data of Fig. 4 of the main text.

S6. Effect of hydrophobic treatment on the bubble profile

The pressure measurement is very sensitive to the presence of a capillary bridge inside the needle, especially in oscillatory measurements. Therefore it was necessary to apply an hydrophobic treatment to the needle as described in the main text. However this has a consequence for the profile of the bubble in the vicinity of the capillary tip (Fig. S7). For an air bubble in water the
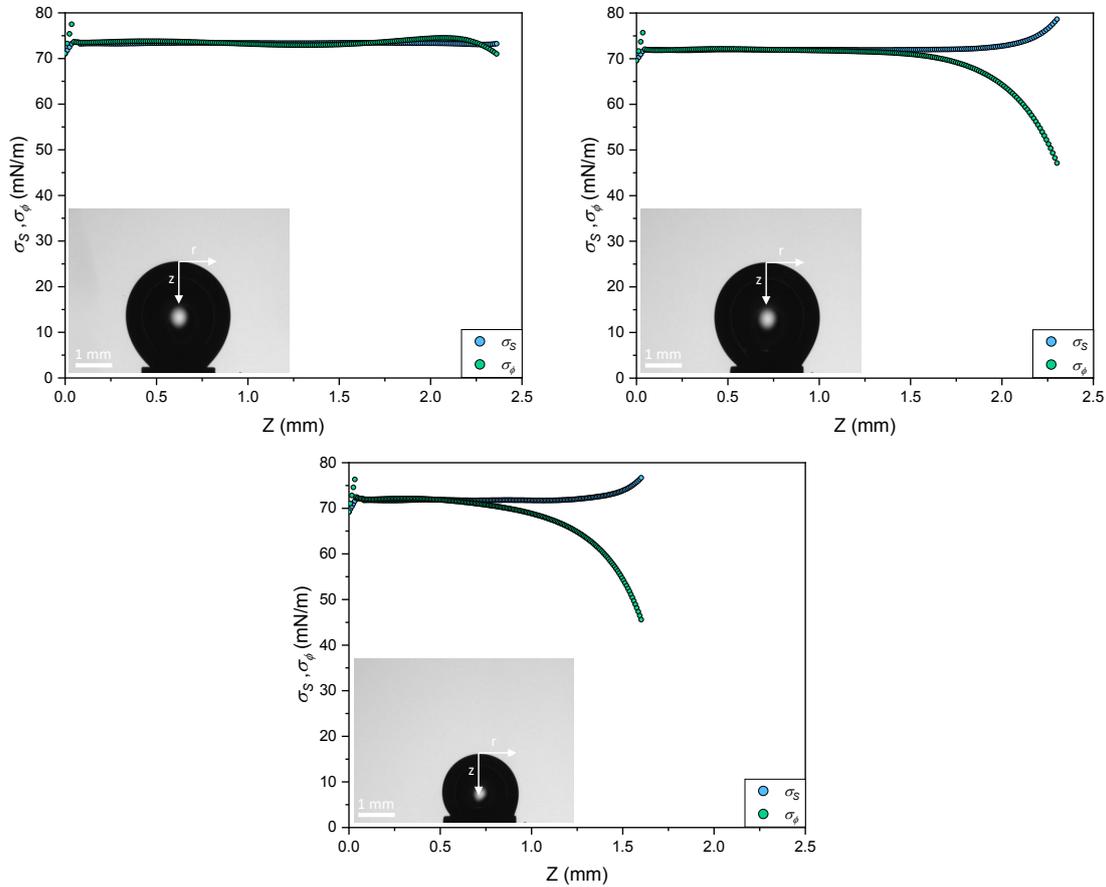

Figure S7. *Effect of hydrophobic treatment on the profile of an air bubble in water analysed by the CMD method: untreated needle (top left) and hydrophobically treated needle (top right). The same perturbation of the profile is observed on the deflated bubble (bottom).*

stresses should be identical and homogeneous. However it is well known that the nature of the capillary has an effect on the accuracy of the fitted surface tension, especially if the Young-Laplace equation is fitted on the profile while including parts too close from the tip.[2] This is simply because the contact line between needle, water and air is not taken into account in the analysis. In the case of an hydrophobic treatment (Fig. S7 top right), the effect of this contact line propagates much further along the profile than without hydrophobic treatment (Fig. S7, top left). When the bubble is deflated, the characteristic length of this effect is not changed and a larger part of the profile is affected (Fig. S7, bottom). To decrease this effect, we rub the tip with sand-paper.

S7. Additional data for the increase of shear moduli with the number of bilayers

Fig. S8 shows the effect of increasing the strain amplitude to 0.3% in the first time sweep instead of 0.08% in the main text. Other tests performed on the sample remain the same as the example in the main text. The resulting average values, calculated as explained in the main text, are shown in Table S1. It is clear that the values of G' and G'' are smaller than in Table 1 (main text) and that the shear amplitude in the initial time sweep is affecting the rheological properties of the bilayers. The Poisson ratio calculated for the 3 bilayers skin is estimated to 0.78 ± 0.09 and reflects the decrease of G' relatively to K'.

(a) Time sweep f: 0.01 Hz, strain amplitude: 0.3%.

(b) Frequency sweep, strain amplitude: 0.08%.
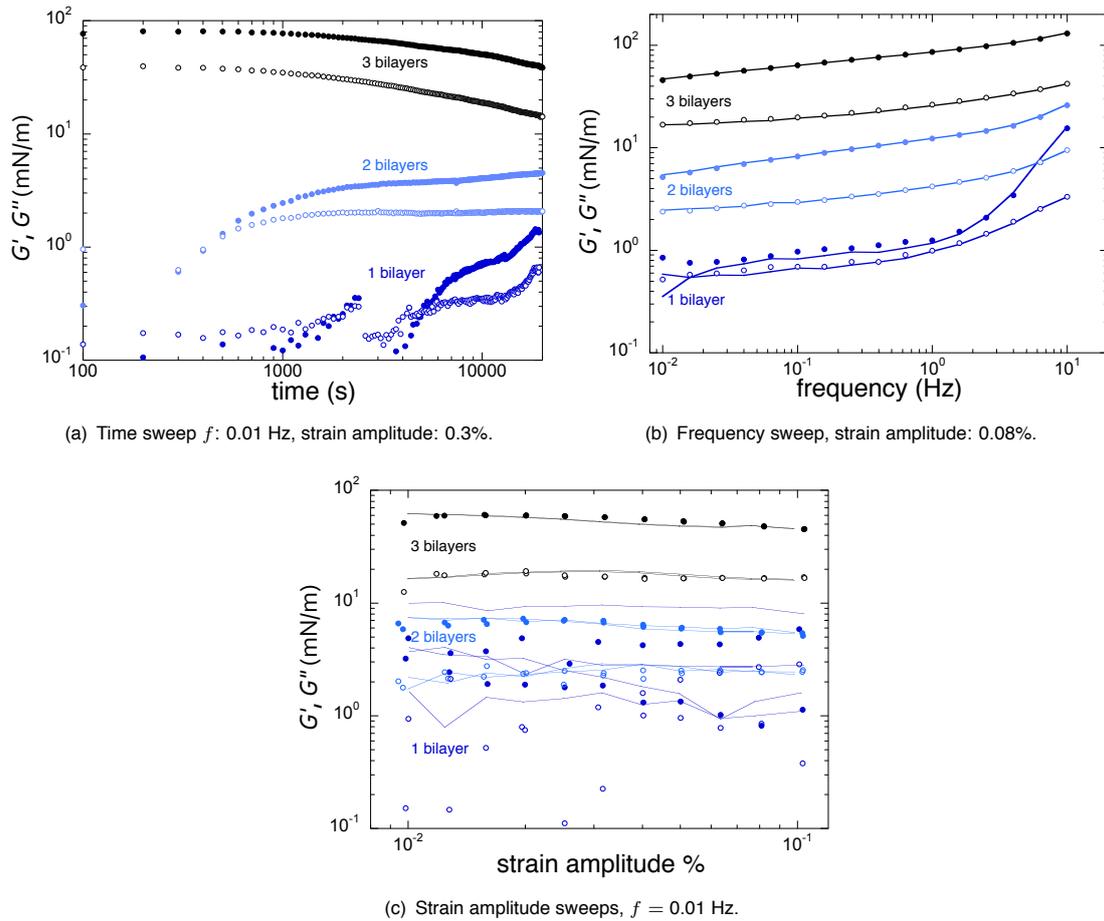

(c) Strain amplitude sweeps, $f = 0.01$ Hz.

Figure S8. *Evolution of the moduli G' (closed symbols) and G'' (open symbols) of the interface as bilayers are progressively added. The first NaPSS layer has relaxed for 120 min before the addition of the first PAH layer.*

Table S1. *Average values for the rheological properties of the multi-layers*

	1 bilayer	2 bilayers	3 bilayers
K' (mN/m)	39±10	181±13	410±21
K'' (mN/m)	2.9±0.5	24±4	99±12
G' (mN/m)	3.2±1.6	6.0±0.3	51±2
G'' (mN/m)	1.3±0.5	2.4±0.1	17.2±0.3
exponent G'	0.14±0.01	0.18±0.01	0.14±0.01
exponent G''	0.11±0.01	0.09±0.01	0.08±0.01

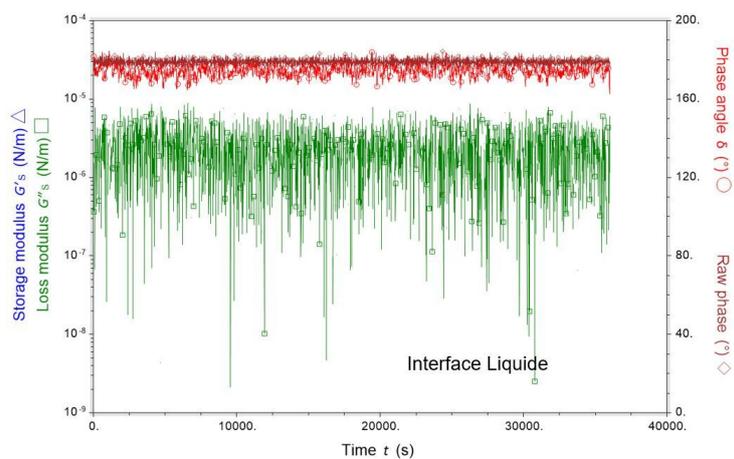## S8. Shear rheology of first NaPSS layer

Figure S9. *Data measured on a first NaPSS layer after 120 min of relaxation. Although the signal is very noisy, it could yield an average value but the value of the raw phase is much too high for an effective correction of the inertia of the apparatus.*

References

[1] O. Théodoly, R. Ober and C. E. Williams, *Eur. Phys. J. E*, 2001, **5**, 51–58.

[2] M. Hoorfar and A. W. Neumann, *Adv. Colloid Interf. Sci.*, 2006, **121**, 25–49.